

Research on the Control of the end Effector of the Large-Scale Curved Surface Compliant Polishing Robot

Runyang Zhan

Ningbo Institute of Technology, Zhejiang University, Ningbo, 315000, China

Keywords: Path Planning, Particle Swarm Optimization, Tuna Swarm Optimization.

Abstract: Curved surface parts find extensive use in various applications, and their surface quality plays a crucial role in their performance. Industrial robot technology has advanced to the point where manual polishing can be replaced. However, most robots currently employ position control, which has low accuracy in force control and is unsuitable for the task. This paper aims to address the limitations of current research by focusing on an improved control strategy that uses a parameter optimization algorithm to enhance the system's dynamic performance. The main areas of research include the control of the end effector's contact force. Firstly, a mathematical model of the pneumatic control loop is established and the system transfer function is obtained through system identification. An improved optimization algorithm based on Particle Swarm Optimization and Tuna Swarm Optimization is proposed to enhance the mechanism's control performance when dealing with complex nonlinear systems. This algorithm has a faster convergence speed, higher convergence accuracy, and stronger searchability.

1 INTRODUCTION

There has been some progress in the research of flat automatic polishing due to the advancements in industrial robot application technology. However, there are still some problems to be solved in the application of robots in the field of large curved surface compliance polishing.

Managing compliance force for large curved surfaces presents a challenging task due to strong coupling, nonlinearities, and frequent changes. The traditional control method's utilization is insufficient to allow for the real-time adaptive adjustment of the control proportional coefficient. This leads to inadequate system performance and the incapability to maintain a stable and consistent force processing target. To enhance the control effect, it is imperative to implement a control strategy that is combined with a parameter optimization algorithm.

In the 21st century, robot technology has emerged as a major high-tech industry that is playing a crucial role in the lives and work of people across the globe. With rapid developments in other industries like automobiles and computers, robots are now widely used in electrical and electronics, automobile, metal and machinery manufacturing, plastics and chemistry,

food and beverage, and other industries. Industrial robots are highly regarded in academia and industry because of their flexibility, excellent motion stability, and high-precision repetitive trajectory motion in a large workspace (Yu 2020). Despite COVID-19's impact on the industry in the first two years, the total number of industrial robots installed worldwide has continued to increase, with a ten-year growth rate of 211%. It is predicted that the number of industrial robots installed globally will exceed 690,000 by 2025.

In today's technological era, using robots for grinding and polishing is more popular than traditional manual methods. This is especially useful for large, curved parts that have complex and uneven surface profiles, requiring precision in both profile and surface finish. Nonetheless, it is worth noting that industrial robots have lower position accuracy and repeatability accuracy when compared to Computer Numerical Control (CNC) machine tools (Zhang 2021). When it is located in different spatial poses, its stiffness difference (Wen & Pagilla 2021) and dynamic characteristic change (Amersdorfer et al. 2020) are relatively large, which will lead to unpredictable processing vibration and structural deformation (Zhu et al. 2022) during the polishing process, and cannot achieve the expected processing target. Therefore, it is necessary to It is considered to

adjust and optimize the sensor technology to monitor the grinding and polishing process by designing and improving the control algorithm.

In recent years, there has been substantial research conducted on the technology of curved surface polishing utilizing robots, both domestically and internationally. Many scholars have analyzed the limitations inherent in the existing tool contact state research and have proposed new and improved methods. For instance, Xie Liujie of South China University of Technology has enhanced the surface material removal depth model, proposing a multi-directional three-dimensional curved surface grinding and polishing optimization cycloidal machining trajectory based on the Angle Based Flattening++ (ABF++) algorithm. This method was verified through experimentation to improve process control (Xie 2018). Furthermore, Zhang Sui of Soochow University has focused on refining the polishing path and process plan and processing Off-axis aspheric mirror elements with good form error (Zhang 2021).

Yalun Wen et al. presented a new 3D path tracking control framework based on the Hermite-Simpson collocation method, which determines the dynamically feasible Cartesian space processing path and the maximum constant translation speed. They built a robot for the 3D path tracking control grinding and polishing experimental platform, which improved the overall performance of the robot grinding and polishing system and met the surface finishing requirements of curved surface parts (Wen & Pagilla 2021). Finally, Manuel Amersdorfer et al. have proposed a method utilizing distance sensor data to create an approximate model of surface topography, replacing the traditional prior model. They have built a free-form surface force-controlled robot automatic polishing system for real-time path tracking, which accurately controls the normal contact force of grinding and polishing (Amersdorfer et al. 2020).

To solve the problems in the above analysis, this paper conducts the following innovative research. Introducing a new parameter optimization algorithm called Improved Tuna Swarm Optimization - Particle Swarm Optimization (ITSO-PSO) combines tuna with particle swarm optimization. This algorithm boasts fast convergence speeds, high precision, and excellent search capabilities. It excels at dynamic tuning of control parameters and performs well on complex nonlinear multivariable systems with minimal overall error.

2 PARAMETER OPTIMIZATION

2.1 Particle Swarm Optimization Algorithm

The Particle Swarm Optimization (PSO) algorithm is a type of swarm intelligence evolutionary algorithm utilized to optimize nonlinear functions. Its creation is credited to James Kennedy, an American psychologist, and Russell Eberhart, an electrical engineer, in 1995 (Kennedy & Eberhart 1995). Taking inspiration from the foraging behavior of birds, the algorithm treats a flock of birds as massless particles. The positions the particles pass through during flight are considered potential solutions to the optimization problem at hand. As particles fly, they search for viable solutions, their velocity and position being the key factors influencing their progress. Further, extend the particle to n-dimensional space, then the position vector $X_i = \{x_1, x_2, \dots, x_n\}$ of particle i in n-dimensional space, and the flight velocity vector $V_i = \{v_1, v_2, \dots, v_n\}$. Choose the suitable fitness calculation function as the test function, assign the initial position and speed to the particle swarm randomly, identify the optimal position of an individual particle and the group of particles at present, evaluate the fitness of the particle, and progressively revise the position and velocity of the swarm until the ultimate position of the particle swarm is attained.

The speed iteration of the classic PSO algorithm is shown in equation (1), and the position iteration is shown in equation (2),

$$\begin{aligned} (V_i^{k+1} = wV_i^k + c_1r_1(P_{best} - X_i^k) + \\ c_2r_2(G_{best} - X_i^k),) \end{aligned} \quad (1)$$

$$X_i^{k+1} = X_i^k + V_i^{k+1}. \quad (2)$$

The equation includes several variables: k denotes the current iteration number of the particle, while w represents the inertia factor, which balances global and local optimization. Additionally, c_1 and c_2 represent learning factors, which reflect individual and group cognitive abilities respectively, and r_1 and r_2 represent random numbers within the range $[0,1]$. Finally, uppercase P_{best} represents the optimal position of a single particle, while uppercase G_{best} represents the optimal position of the entire particle group.

To initiate the PSO algorithm process, the first step entails initializing the particle swarm. This includes randomly generating the starting position and velocity, as well as selecting appropriate values for the number of iterations, population size, particle dimension, inertia factor, and learning factor. In the subsequent step, a fitness function is adopted and

employed to compute the fitness value of each particle. The third step involves updating each particle by comparing its fitness with its historical optimal value. The fourth step involves updating the particle swarm by comparing each particle's fitness with its historical optimal value. In the fifth step, the velocity and position of the particles are updated according to equations (1) and (2). Finally, the loop end condition is evaluated to determine if it has been met. If not, the process returns to step 2 and continues to execute.

2.2 Tuna Swarm Optimization Algorithm

The Tuna Optimization Algorithm (TSO) is a global meta-heuristic optimization algorithm that simulates

$$Y_j^{k+1} = \begin{cases} \alpha_1 \cdot (Y_{rand}^k + \beta \cdot |Y_{rand}^k - Y_j^k|) + \alpha_2 \cdot Y_j^k, k = 1; rand < \frac{k}{m} \\ \alpha_1 \cdot (Y_{rand}^k + \beta \cdot |Y_{rand}^k - Y_j^k|) + \alpha_2 \cdot Y_{j-1}^k, k \in [2, m]; rand < \frac{k}{m} \\ \alpha_1 \cdot (Y_{best}^k + \beta \cdot |Y_{best}^k - Y_j^k|) + \alpha_2 \cdot Y_j^k, k = 1; rand \geq \frac{k}{m} \\ \alpha_1 \cdot (Y_{best}^k + \beta \cdot |Y_{best}^k - Y_j^k|) + \alpha_2 \cdot Y_{j-1}^k, k \in [2, m]; rand \geq \frac{k}{m} \end{cases} \quad (4)$$

The calculation equation of each coefficient is

$$\alpha_1 = \alpha_0 + (1 - \alpha_0) \cdot \frac{k}{m} \quad (5)$$

$$\alpha_2 = (1 - \alpha_0) - (1 - \alpha_0) \cdot \frac{k}{m} \quad (6)$$

$$\beta = e^{\beta_0 \cdot l} \cdot \cos(2\pi\beta_0), \quad (7)$$

$$l = e^{3 \cos\left(\left(\frac{m+1}{k}\right) - 1\right)\pi}, \quad (8)$$

where Y_j^{k+1} indicates the position of the j th particle after the $(k+1)$ th iteration; Y_{best}^k indicates the position of the current optimal particle; the subscripts α_1 and α_2 refer to weight coefficients that influence a particle's movement towards the optimal particle and its previous trend, respectively. These coefficients effectively control the particle's ability to conduct both global and local searches; α_0 indicates the degree to which the particle follows the optimal particle and the previous article in the initial state; k indicates the current iteration number; m indicates the

the spiral and parabolic foraging behaviors of tuna in a swarm-based approach (Xie et al. 2021). Tuna employs distinct foraging methods, namely the spiral and parabolic techniques. The spiral approach involves swimming in an upward spiral to contain their prey in a confined area for more efficient feeding, while the parabolic technique entails chasing the tuna in front of them to create a parabolic shape for capturing prey. As for initializing particles for the TSO algorithm, a precise calculation equation is implemented,

$$Y_{j0} = rand \cdot (b_{max} - b_{min}) + b_{min}, \quad (3)$$

where Y_{j0} represents the initial position of the tuna, and b_{max} and b_{min} represent the maximum and minimum values of the search range. Further, the position of the tuna population during spiral foraging can be deduced,

maximum The number of iterations; β represents the coefficient of the particle and the optimal particle or random particle, β_0 represents the random number in the value range $[0,1]$; l represents the coefficient related to the maximum number of iterations m and the current number of iterations k , there is no actual physical meaning.

It is assumed that when feeding, tuna has a 50% chance of choosing a parabolic path and a 50% chance of feeding randomly. The mathematical model is

$$Y_j^{k+1} = \begin{cases} Y_{best}^k + rand \cdot (Y_{best}^k - Y_j^k) + q \cdot p^2 \cdot (Y_{best}^k - Y_j^k), rand < 0.5 \\ q \cdot p^2 \cdot Y_j^k, rand \geq 0.5 \end{cases}, \quad (9)$$

$$p = \left(1 - \frac{k}{m}\right)^{\frac{k}{m}}, \quad (10)$$

where the value of q is $\{-1,1\}$, which determines the direction of the particle swarm foraging; p reflects the process of foraging.

2.3 Improved Optimization Algorithm Based on Tuna and Particle Swarm Optimization

When tackling intricate problems with numerous dimensions, the conventional PSO algorithm may present a few limitations. While it boasts a rapid search space velocity, it lacks local search capabilities, causing the optimization to potentially

settle into a local optimum. Furthermore, insufficient information exchange between particles may lead to sluggish convergence, hindering the attainment of the optimal solution (Song et al. 2021). The ITSO-PSO algorithm combines the advantages of both algorithms to enhance global and local search performance.

The speed and position iterative calculation equations of the ITSO-PSO optimization algorithm are

$$\mathbb{V}_g^{t+1} = \begin{cases} w\mathbb{V}_g^t + c_1r_1(M_{best} - Z_g^t) + c_2r_2(M_{best} - Z_g^t), & rand < \frac{t}{maxgen} \\ w\mathbb{V}_g^t + c_1r_1(M_{best} - Z_g^t) + c_2r_2(G_{best} - Z_g^t), & rand \geq \frac{t}{maxgen} \end{cases}, \quad (11)$$

$$Z_g^{t+1} = \begin{cases} w \cdot Z_g^t + w \cdot \mathbb{V}_g^{t+1}, & rand < \frac{t}{maxgen} \\ w \cdot Z_g^t + (1 - w) \cdot \mathbb{V}_g^{t+1}, & rand \geq \frac{t}{maxgen} \end{cases}, \quad (12)$$

$$M_{best} = \frac{P_{best} + G_{best}}{2}, \quad (13)$$

where \mathbb{V}_g^{t+1} and Z_g^{t+1} represent the speed and position of the g th particle after the $(t+1)$ iteration, $maxgen$ represents the maximum number of iterations, and M_{best} represents the particle's personal best position and group best position average.

The optimization capabilities of a particle swarm are influenced by the inertia factor and the learning factor. A larger inertia factor means weaker local optimization capabilities, while a smaller one leads to

weaker global optimization. When the learning factor c_1 is small, particles may struggle with local search and become stuck in suboptimal situations, unable to reach the global optimal solution. Similarly, when c_2 is small, particles may not communicate enough, slowing down convergence and preventing the discovery of an optimal solution. Therefore, it is necessary to properly improve and optimize the inertia factor and learning factor (Zhao et al. 2014), and the changes are

$$w = 0.5 \cdot (w_s + w_e) + 0.5 \cdot (w_s - w_e) \cdot \tanh\left(-4 + \frac{8 \cdot (maxgen - t)}{maxgen}\right), \quad (14)$$

$$c_1 = c + (c_1 - c) \cdot \frac{t}{maxgen}, \quad (15)$$

$$c_2 = (c - 0.5) + (c - c_2) \cdot \frac{t}{maxgen}, \quad (16)$$

where w_s and w_e represent the initial value and final value of the inertia factor respectively.

To begin the ITSO-PSO algorithm, several parameters must be initialized, including the learning factor, inertia weight, maximum evolution times, population size, and fitness function dimension. Additionally, the value range of speed and position must be limited and a fitness function must be selected. Following this, a population is randomly generated and the speed and fitness of each particle are calculated. The best fitness values of the individual and the group are then calculated and updated accordingly. The algorithm then iteratively updates the inertia factor, learning factor, particle swarm velocity, and position using a *ala* while preventing them from exceeding their range. To avoid getting stuck at a local optimum, mutation seeds are

added. The algorithm continues until the end condition is met, at which point the descending optimization curve is output.

2.4 ITSO-PSO Algorithm Performance Test

To compare the effectiveness of the ITSO-PSO algorithm with the PSO algorithm, we selected five classic test functions and conducted comparative testing to verify the performance change (Huang et al. 2018). In total, there are five test functions. Two of them are unimodal test functions called Sphere and Schwefel's Problem 2.22, which aid in determining the algorithm's search accuracy and iteration rate. The remaining three tests are multimodal test functions - Griewank, Ackley, and Rastrigin - designed to

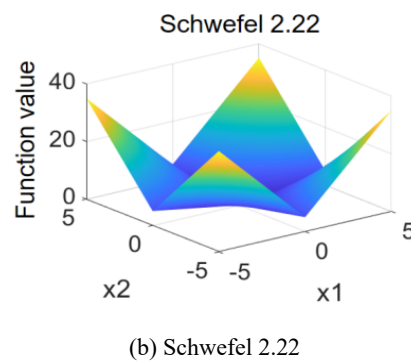
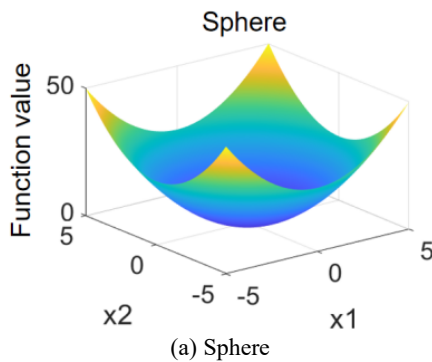
prevent the algorithm from converging prematurely by avoiding local optima. Table 1 provides the optimal values and value ranges for all five test functions, while Figure 1 visually represents the definition domain and value range of the test functions in three dimensions.

Use MATLAB R2019b version for code writing and simulation testing, set the maximum number of population iterations $maxgen=200$; population size $G=100$; inertia weight correlation coefficient $w=0.9$, $w_s =0.9$, $w_e =0.4$; learning factor correlation coefficient $c=1.5$, $c_1=1.49345$, $c_2=1.44345$; set the speed value range $[-1,1]$; set the position range according to Table 1. After defining the initial

parameters, a specific test function is selected, and varying variable dimensions are independently tested for both algorithms, with each test run 30 times. For each test where the fitness function converges (i.e. when the fitness value is less than 0.001), the average (AVG), standard deviation (STD), maximum (MAX), minimum (MIN), and mean (MEAN) number of iterations are documented. In cases where the number of iterations is 200 and the fitness value is greater than or equal to 0.001, the function is classified as not having converged, and MAX, MIN, and MEAN are marked as DNE. The outcomes of each test are meticulously analyzed and documented in Table 2, Table 3, Table 4, Table 5, and Table 6.

Table 1: The basic situation of 5 classic test functions.

Name	Equation	Range	Optimal value
Sphere	$f_1 = \sum_{i=1}^N (x_i)^2$	$[-100,100]$	0
Schwefel 2.22	$f_2 = \sum_{i=1}^N x_i + \prod_{i=1}^N x_i $	$[-10,10]$	0
Griewank	$f_3 = \frac{1}{4000} \sum_{i=1}^N (x_i)^2 - \prod_{i=1}^N \cos\left(\frac{x_i}{\sqrt{i}}\right) + 1$	$[-600,600]$	0
Ackley	$f_4 = -20 \cdot \exp\left(0.2 \cdot \sqrt{\frac{1}{N} \sum_{i=1}^N (x_i)^2}\right) - \exp\left(\frac{1}{N} \sum_{i=1}^N \cos(2\pi x_i)\right) + 20 + e$	$[-32,32]$	0
Rastrigin	$f_5 = \sum_{i=1}^N [x_i^2 - 10 \cos(2\pi x_i) + 10]$	$[-5.12,5.12]$	0



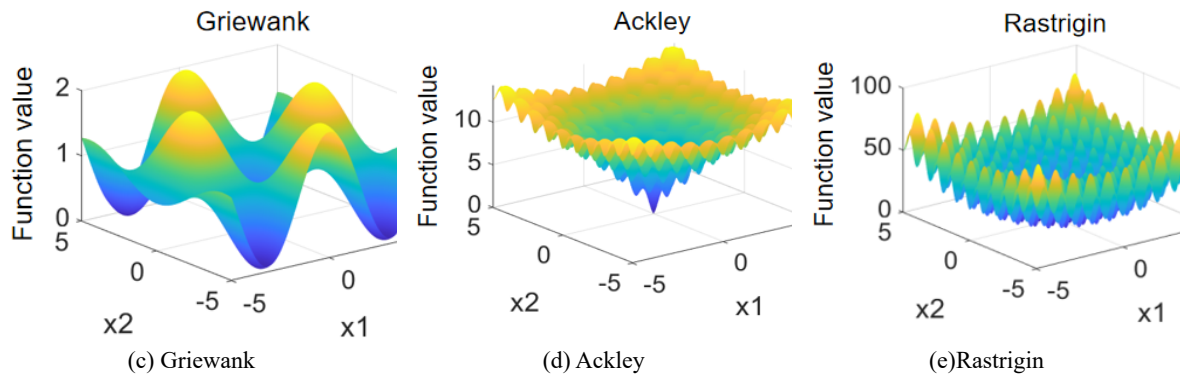


Figure 1: 3D visualization output of test function.

Table 2: Comparison of 2 optimization algorithms for solving 5 test functions (variable dimension D=3).

Algorithm	Index	f_1	f_2	f_3	f_4	f_5
ITSO-PSO	AVG	0	0	0	0	0
	STD	0	0	0	0	0
	MAX	55	99	56	100	82
	MIN	32	91	31	94	51
	MEAN	46	95	44	98	66
PSO	AVG	0	0	0	0	0.13329
	STD	0	0	0	0	0.33935
	MAX	81	143	72	141	196
	MIN	57	111	62	112	39
	MEAN	73	128	67	130	110

Table 3: Comparison of 2 optimization algorithms for solving 5 test functions (variable dimension D=10).

Algorithm	Index	f_1	f_2	f_3	f_4	f_5
ITSO-PSO	AVG	0	0	0	0	0
	STD	0	0	0	0	0
	MAX	81	108	72	106	128
	MIN	71	103	62	102	83
	MEAN	76	106	68	104	89
PSO	AVG	0	0.00395	0	0.00093	5.98740
	STD	0	0.00662	0	0.00007	3.40882
	MAX	138	200	140	137	DNE
	MIN	109	119	104	96	DNE
	MEAN	126	169	119	114	DNE

Table 4: Comparison of 2 optimization algorithms for solving 5 test functions (variable dimension D=30).

Algorithm	Index	f_1	f_2	f_3	f_4	f_5
ITSO-PSO	AVG	0	0	0	0	0
	STD	0	0	0	0	0
	MAX	88	112	80	109	99
	MIN	84	110	74	106	95
	MEAN	86	111	77	108	96
PSO	AVG	0.00096	0.27348	0.00097	0.01208	23.64657
	STD	0.00004	0.09489	0.00003	0.00351	9.75532
	MAX	191	DNE	134	DNE	DNE
	MIN	138	DNE	91	DNE	DNE
	MEAN	168	DNE	115	DNE	DNE

Table 5: Comparison of 2 optimization algorithms for solving 5 test functions (variable dimension D=50).

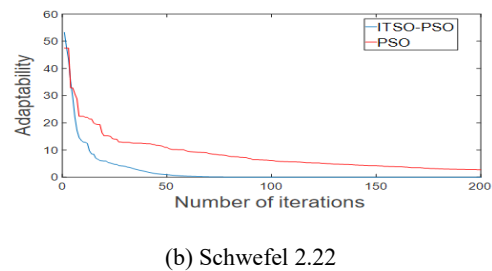
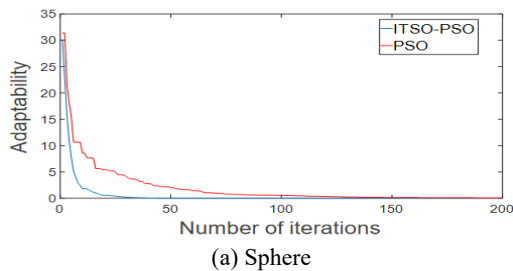
Algorithm	Index	f_1	f_2	f_3	f_4	f_5
ITSO-PSO	AVG	0	0	0	0	0
	STD	0	0	0	0	0
	MAX	90	114	82	109	99
	MIN	86	111	75	107	97
	MEAN	88	112	78	108	98
PSO	AVG	0.00723	0.91041	0.00098	0.05423	40.34964
	STD	0.00207	0.17174	0.00002	0.00980	14.06941
	MAX	DNE	DNE	192	DNE	DNE
	MIN	DNE	DNE	154	DNE	DNE
	MEAN	DNE	DNE	169	DNE	DNE

Table 6: Comparison of 2 optimization algorithms for solving 5 test functions (variable dimension D=100).

Algorithm	Index	f_1	f_2	f_3	f_4	f_5
ITSO-PSO	AVG	0	0	0	0	0
	STD	0	0	0	0	0
	MAX	92	115	82	109	100
	MIN	87	113	77	106	98
	MEAN	89	114	79	108	99
PSO	AVG	0.07823	2.64485	0.00169	0.14961	177.16030
	STD	0.01089	0.22698	0.00023	0.01661	47.02125
	MAX	DNE	DNE	DNE	DNE	DNE
	MIN	DNE	DNE	DNE	DNE	DNE
	MEAN	DNE	DNE	DNE	DNE	DNE

Based on the simulation results outlined in the table, it's clear that both algorithms can achieve iterative test value convergence when the variable dimension is low. However, the traditional PSO algorithm requires more iterations, and as the variable dimension increases, some of its test functions fail to converge. If the variable dimension reaches a critical point, the PSO algorithm won't converge, and each evaluation performance indicator parameter will decline to varying degrees. By analyzing the change curves of the five test degree functions shown in Figure 2, we can see that the proposed ITSO-PSO optimization algorithm can

achieve the theoretical optimal solution in all test scenarios, meaning that the test function can converge in any scenario. Compared to the traditional PSO algorithm, the ITSO-PSO algorithm achieves convergence with fewer iterations, indicating a faster convergence rate. Additionally, the ITSO-PSO algorithm is more robust, even when the variable dimension increases from 100 to 500. The average number of convergence times when the algorithm reaches convergence does not increase significantly, making numerical variable space parameter optimization a valuable reference point, as shown in Figure 3.



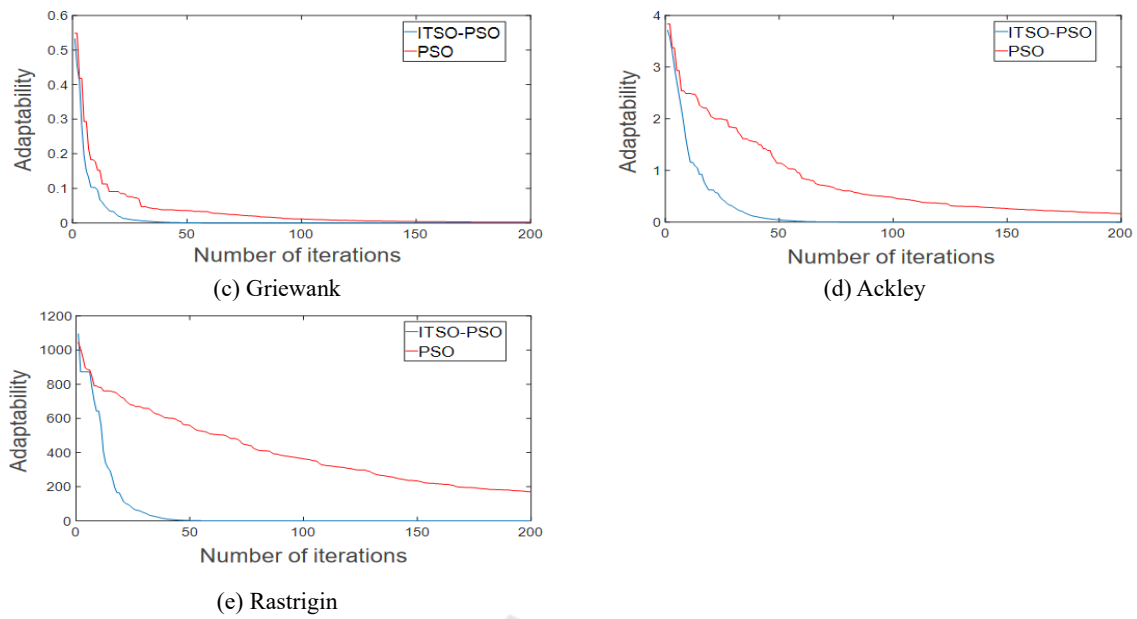


Figure 2: Five test function fitness change curves (D=100).

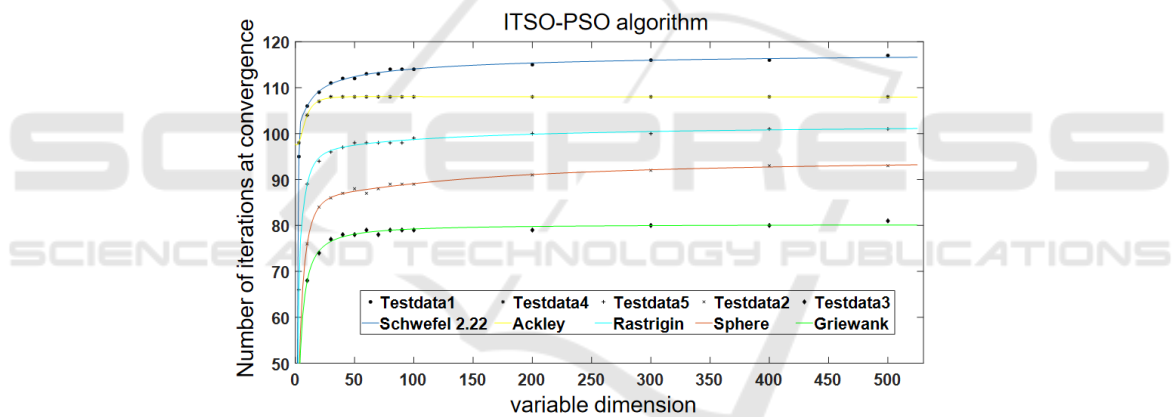


Figure 3: ITSO-PSO algorithm convergence times and variable dimension function curve.

In summary, the ITSO-PSO algorithm proposed based on the TSO algorithm and the traditional PSO algorithm solves the problem of premature convergence that may fall into local extreme points when solving complex nonlinear unimodal or multimodal function problems. The test results show that the ITSO-PSO algorithm has a fast convergence speed, good global search ability and local search ability, high convergence accuracy, and the ability to optimize complex system parameters.

3 CONCLUSION

This paper centers around the precise manipulation of the end effector on a polishing robot, specifically one designed for curved surfaces. This paper has yielded remarkable results thus far. This paper developed a mathematical model that enables me to establish a pneumatic control loop for each component and pinpoint the transfer function of the pneumatic control system. Ther proposed ITSO-PSO algorithm has outperformed traditional PSO algorithms in terms of faster convergence speed, increased accuracy, and superior capabilities for both global and local searches. Although the research has its limitations,

there is potential for future development using machine vision technology to track and monitor the robot's polishing path and surface processing in real time. This could enhance the system's intelligence to a higher level.

dynamically adjusting inertial weights”, *Small and Micro Computer Systems*, 2018, 39(12): 2590-2595.

REFERENCES

- H. Yu, “Optimal design and experimental research of industrial robot end grinding tool”, Jilin University, 2020.
- S. Zhang, “Research on off-axis aspheric wheel polishing technology based on industrial robots”, Soochow University, 2021.
- Y. Wen and P R. Pagilla, “A novel 3D path following control framework for robots performing surface finishing tasks”, *Mechatronics*, 2021, 76: 102540.
- M. Amersdorfer, J. Kappey and T. Meurer, “Real-time freeform surface and path tracking for force controlled robotic tooling applications”, *Robotics and Computer-Integrated Manufacturing*, 2020, 65: 101955.
- Z. Zhu, X W. Tang, C. Chen, F Y. Peng, R. Yan, L. Zhou, Z P. Li and J W. Wu, “High precision and efficiency robotic milling of complex parts: Challenges, approaches and trends”, *Chinese Journal of Aeronautics*, 2022, 35(2): 22-46.
- L J. Xie, “Tool contact state analysis and multi-directional trajectory process control for robot surface polishing”, South China University of Technology, 2018.
- S. Zhang, “Research on off-axis aspheric wheel polishing technology based on industrial robots”, Soochow University, 2021.
- Y. Wen and P R. Pagilla, “A novel 3D path following control framework for robots performing surface finishing tasks”, *Mechatronics*, 2021, 76: 102540.
- M. Amersdorfer, J. Kappey and T. Meurer, “Real-time freeform surface and path tracking for force controlled robotic tooling applications”, *Robotics and Computer-Integrated Manufacturing*, 2020, 65: 101955.
- J. Kennedy and R. Eberhart, “Particle swarm optimization,” Proceedings of ICNN'95 - International Conference on Neural Networks, Perth, WA, Australia, 1995, pp. 1942-1948 vol.4, doi: 10.1109/ICNN.1995.488968.
- L. Xie, T. Han, H. Zhou, Z R. Zhang, B. Han and A. Tang, “Tuna Swarm Optimization: A Novel Swarm-Based Metaheuristic Algorithm for Global Optimization”, *Computational Intelligence and Neuroscience*, 2021, 2021: 9210050.
- B Y. Song, Z D. Wang and L. Zhou, “An improved PSO algorithm for smooth path planning of mobile robots using continuous high-degree Bezier curve”, *Applied Soft Computing*, 2021, 100: 106960.
- Z G. Zhao, S Y. Huang and W Q. Wang, “Simplified particle swarm optimization algorithm based on random inertial weights”, *Computer Application Research*, 2014, 31(02): 361-363.
- Y. Huang, H Y. Lu, K B. Xu and W Q. Shen, “A simplified mean particle swarm optimization algorithm for